A theoretical compartment model for antigen kinetics in the skin

Anne M. Römgens[a], Dan L. Bader[a,b], Joke A. Bouwstra[c], Cees W.J. Oomens[a]

[a]Soft Tissue Biomechanics and Engineering, Department of Biomedical Engineering, Eindhoven University of Technology, P.O. Box 513, 5600 MB Eindhoven, the Netherlands.
[b]Faculty of Health Sciences, University of Southampton, Southampton SO17 1BJ, UK.
[c]Division of Drug Delivery Technology, Leiden Academic Centre for Drug Research, Leiden University, P.O. Box 9502, 2300 RA Leiden, the Netherlands.

Corresponding author: A.M. Römgens, Soft Tissue Biomechanics and Engineering, Department of Biomedical Engineering, Eindhoven University of Technology, PO Box 513, 5600 MB Eindhoven, The Netherlands. Tel.: +31402475415, E-mail address: a.m.romgens@tue.nl

Abstract

The skin is a promising location for vaccination with its abundant population of antigen capturing and presenting cells. The development of new techniques, such as the use of microneedles, can facilitate the delivery of vaccines into the skin. In recent years, many different types of microneedle arrays have been designed. However, their geometry and arrangement within an array may be optimized to trigger sufficient antigen presenting cells. A computational model can support the rational design of microneedle arrays. Therefore, the aim of the current study was to describe the distribution and kinetics of a delivered antigen within the skin using a theoretical compartment model, which included binding of antigens to receptors and their uptake by cells, and to determine which parameters should be measured to validate the model for a specific application. Multiple simulations were performed using a high and low antigen delivery dose and a range of values for the rate constants. The results indicated that the cells were highly saturated when a high dose was applied, while for a low dose saturation was only reached in 5% of the simulations. This was caused by the difference in the ratio between the administered dose and the available binding sites and suggests the dose should be adapted to the number of cells and receptors for a specific compound. The sensitivity analysis of the model parameters confirmed that the initial dose and receptor concentrations were indeed the two parameters that had the largest influence on the variance in antigen concentrations within the cells and circulation at equilibrium. Hence, these parameters are important to be measured in vivo. The presented pharmacokinetics model can be used in future computational models to predict the influence of microneedle array geometry to optimize their design.

Keywords: Pharmacokinetic model; Antigen uptake; Skin kinetics; Vaccine delivery

1. Introduction

Vaccines are traditionally delivered to subcutaneous or intramuscular tissues with a hypodermic needle and syringe. However, recent studies have reported that skin is a promising target for vaccine administration, since it is rich with antigen presenting cells (APCs), such as Langerhans cells and dermal dendritic cells (Al-Zahrani et al., 2012; van der Maaden et al., 2012). When an antigen is delivered in the epidermis and dermis, it will diffuse through the different skin layers (Raphael et al., 2013; Römgens et al., 2015). One of these layers, the viable epidermis, is mainly composed of keratinocytes, but also contains a large population of Langerhans cells (Koutsonanos et al., 2013). Beneath the epidermis lies the dermis, a relatively thick layer rich in collagen fibres. Among others, dermal dendritic cells reside in the dermis. After antigens are delivered into the skin, three options are possible:

1. They can be recognized, bind and be internalized by the cells residing in the skin (Giese, 2013; Koutsonanos et al., 2013). This uptake of antigens occurs by receptor-mediated endocytosis or by fluid phase pinocytosis (Abbas et al., 2012; Mizuno et al., 2004). Multiple receptors, such as Toll-like receptors and C-type receptors, play a role in the specific binding and internalization of antigens (Dzopalic et al., 2012; Flacher et al., 2006; Mizuno et al., 2004; Ueno et al., 2007). After internalization of antigens, the two populations of antigen presenting cells will mature and start to migrate towards the draining lymph nodes (Dzopalic et al., 2012). There, they present the processed antigens to T-cells, which initiates an adaptive immune response (Koutsonanos et al., 2013). The response mechanism of the APCs in the skin is influenced by the secretion of various signal molecules such as cytokines and chemokines (Koutsonanos et al., 2013), which are secreted by other skin cells, such as keratinocytes (Flacher et al., 2006), as a response to antigen encounter and other chemical and physical triggers.
2. Antigens can directly diffuse to the lymph nodes and activate the lymph node-resident dendritic cells (Abbas et al., 2012; Ueno et al., 2007).
3. Antigens can be transported away from the skin by uptake in the systemic circulation through the capillaries within the dermis.

To deliver antigens into the skin, microneedles are being developed. These microneedles are small projections that are often arranged in an array and are used to bypass the stratum corneum, which is impermeable to larger molecules (Bos and Meinardi, 2000). Microneedles can be hollow to inject a fluid, solid to make conduits in the skin, coated with an antigen or made of a dissolvable material containing the antigen (van der Maaden et al., 2012).

Although many microneedle types are now available, involving different types, geometries, and arrangements in an array (Indermun et al., 2014; Kim et al., 2012), little is known about their specific

influences on the delivery and transport of the antigen and thus the effectiveness of the immune response. One of the few studies using coated microneedles reported that the immune response is mostly independent on the microneedle array geometry (Widera et al., 2006). By contrast, another study revealed an effect of microneedle array density on the immune response (Depelsenaire et al., 2014). In addition, the total volume of the microneedles on an array has been reported to influence the immune response when topically applying an antigen before treating the skin with microneedles (Carey et al., 2011; Pearson et al., 2015). These results suggest that the potency of the immune response may vary depending on the microneedle array geometry. To optimize microneedle array designs, it would be beneficial to develop a computational model which predicts the influence of various features of the microneedles on the resulting efficiency of the immune response.

A first step in this process would be a model to describe the transport within the skin. Mathematical models have previously been used to predict the transport of topically applied drugs through the skin and into the circulation, as reviewed by Mitragotri and coworkers (Mitragotri et al., 2011), and Naegel and coworkers (Naegel et al., 2013). Models can be separated into those that consider the spatial distribution inside the skin (e.g. Dancik et al., 2012; Kretsos et al., 2008) and those considering the average concentration in various compartments of the skin (e.g. McCarley and Bunge, 2001). Both models have been developed on the macroscopic (tissue) and microscopic (cell) levels, where aspects such as metabolic activity, binding to skin components, diffusion and partitioning are considered. In addition, some models focused on the transport through the skin after drug administration with microneedles (Al-Qallaf et al., 2009; Kim et al., 2015; Lv et al., 2006; Zhang et al., 2009). Most of these models focus on transport to the systemic circulation, as opposed to kinetics within the skin. However, for vaccination purposes it is the latter which is critical, involving events such as the binding of antigens to receptors and their internalization by dendritic cells. For example, receptor mediated endocytosis can be included, which has been modelled at the microscopic level (Gex-Fabry and DeLisi, 1984).

The aim of the present study was to (1) develop a model that described the distribution of an antigen within different components of the skin and included the binding and internalization of the antigen by cells residing in the skin. (2) To determine which parameters should be accurately measured in an in vivo setup, because they demonstrate the largest influence on variation in equilibrium concentrations. This was achieved by developing a theoretical compartment (pharmacokinetic) model of the skin and its cells and by performing a sensitivity analysis on the model parameters, which were taken from those reported in the literature. This analysis was designed to determine which parameters should be measured accurately for a more precise output, providing a template to perform validation experiments which match specific applications.

2. Methods

2.1 Theoretical compartment model of skin kinetics

To describe the distribution of an antigen delivered to the skin, a theoretical compartment model was developed. In this type of model, the average concentration in a single compartment is considered as opposed to calculating the spatial concentration distribution. The present study extended a basic compartment (pharmacokinetic) model of the skin (McCarley and Bunge, 2001) with both a compartment representing antigens bound to receptors on the cell membrane and a compartment of the intracellular space. It was assumed that antigen uptake by cells only occurred via receptor-mediated endocytosis. The compartment model consisted of five compartments (Fig. 1), which are defined as follows:

- The microneedle (MN), or other delivery device
- The extracellular matrix of the skin (ECM)
- The receptors on the cell (rec)
- The intracellular space (cells)
- The blood and lymph circulation (circ)

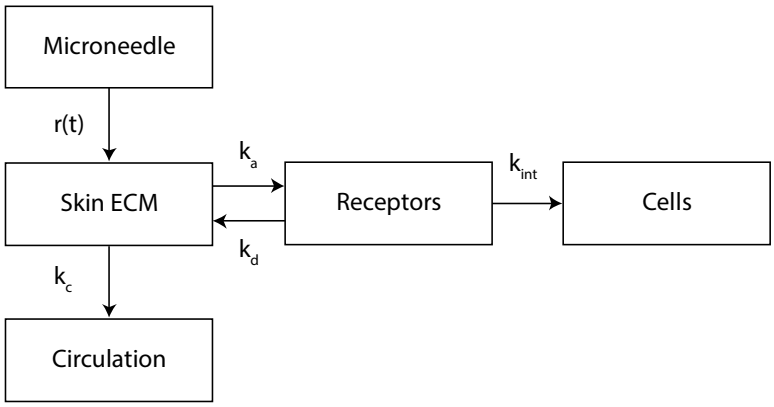

Figure 1. Compartment model to describe the kinetics of antigens delivered into the skin. The concentration of an antigen in the extracellular matrix, bound to receptors on the cell membranes, inside the cells and in the circulation is determined by the release from the microneedle r and the exchange of antigens between the various compartments. This exchange is dependent on the rates k_β.

The change in concentration of the antigen within or bound to these various compartments was described with a set of differential equations (eqs. (1)-(5)):

$$\frac{dC_{MN}(t)}{dt} = -r(t), \tag{1}$$

$$\frac{dC_{ECM}(t)}{dt} = r(t) - k_a C_{ECM}(t)\big(R_{tot} - C_{rec}(t) - C_{cells}(t)\big) + k_d C_{rec}(t) - k_c C_{ECM}(t), \tag{2}$$

$$\frac{dC_{rec}(t)}{dt} = k_a C_{ECM}(t)\big(R_{tot} - C_{rec}(t) - C_{cells}(t)\big) - (k_d + k_{int})C_{rec}(t), \tag{3}$$

$$\frac{dC_{circ}(t)}{dt} = k_c C_{ECM}(t), \tag{4}$$

$$\frac{dC_{cells}(t)}{dt} = k_{int} C_{rec}(t), \quad (5)$$

where C_α represents the antigen concentration in the different compartments with α = MN, ECM, circ, and cells; C_{rec} the concentration of antigens bound to the receptors; r the release rate from the microneedle; k_a and k_d indicate the association and dissociation rate constant of the antigens to bind to the receptors, respectively; k_{int} the rate of internalization of the antigen-receptor complex into the cell; k_c the rate of uptake into the circulation; R_{tot} the total initial concentration of receptors on the cell membranes; and t the time.

The change in concentration in the microneedle compartment (eq. (1)) was determined by the release rate of antigens to the extracellular matrix. In the model, a constant release of antigen from the microneedle was assumed for a specific release period t_r, as prescribed by eq. (6).

$$r(t) = \begin{cases} \frac{C_{MN,0}}{t_r} & 0 > t \geq t_r \\ 0 & t > t_r \end{cases}, \quad (6)$$

where $C_{MN,0}$ is the initial concentration in the microneedle.

The released antigens enter the ECM compartment changing its concentration (first term, right-hand side of eq. 2). From this compartment, antigens can move to the receptor compartment and antigens that previously moved to the receptor compartment can move back to the ECM (Fig. 1). This equilibrium was prescribed with the following chemical reaction:

$$C_{ECM} + R_f \underset{k_d}{\overset{k_a}{\rightleftarrows}} C_{rec}, \quad (7)$$

where R_f is the concentration of free receptors. Hence, the rate of antigen binding to receptors was prescribed as follows:

$$\left.\frac{dC_{ECM}}{dt}\right|_{binding} = -k_a C_{ECM}(t) R_f, \quad (8)$$

It was assumed that the receptors could not be recycled, hence each receptor can facilitate the uptake of a single antigen into the cells. Consequently, the concentration of free receptors (R_f) is equal to the initial receptor concentration (R_{tot}) minus the concentration of antigens bound to the receptors (C_{rec}) and antigens in the intracellular space (C_{cells}). This in combination with eq. (8) results in the second term on the right-hand side of eq. (2). The third term describes the release of antigens from the receptor compartment. The antigens can also be taken up into the circulation, which is accounted for with the fourth term of eq. (2).

The concentration in the receptor compartment increases due to binding of antigens to the receptors (first term, right-hand side of eq. (3)). In addition, the antigen-receptor complex can, subsequently, be

taken up in the cell compartment or be released to the ECM compartment (second term, right-hand side of eq. (3)). Once an antigen was taken up in a cell or the circulation it could not move to another compartment, as represented by eq. (4) and (5).

The mathematical model was implemented in Matlab (2013a, The MathWorks, Inc., Natick, MA, USA) to numerically solve the set of differential equations and, thereby, determine the concentration change with time and the equilibrium concentrations of the compartments. Simulations were run until the equilibrium was attained according to three inclusive criteria. The concentration of antigens bound to receptors ($\mathrm{C_{rec}}$) and the concentration in the ECM ($\mathrm{C_{ECM}}$) should be smaller than 0.001% of the total concentration of receptors ($\mathrm{R_{tot}}$) and total concentration of antigens ($\mathrm{C_{MN,0}}$), and the relative change in concentration in the cells ($\mathrm{C_{cells}}$) should be less than 0.001%. For simplicity, it was assumed that all compartments had an equal volume.

2.2 Input for model parameters to describe kinetics

2.2.1 Rate constants

The kinetics model prescribed in the previous section required 7 parameters as input, including four rate constants. These rate constants k_β were not known for a specific antigen of interest, and thus a range of values per rate constant were employed, as indicated in Table 1.

2.2.2 Initial concentration of receptors

The initial concentration of antigen binding receptors (R_{tot}) was based on the number of receptors per cell N_{rec} and the cell density N_{cell} in the epidermis and dermis. The number of Langerhans cells and dermal dendritic cells has often been measured as cells per mm^2 (Table 1). To convert this surface density to cells per mm^3 the following equation was used, assuming a homogeneous cell distribution and cellular dimensions that are the same in all dimensions:

$$N_{cell} = n_{cell}\sqrt{n_{cell}}\,, \tag{9}$$

where $N_{cell,l}$ is the cell density in cells/mm^3 and $n_{cell,l}$ the cell density in cells/mm^2. Using eq. (9) and assuming a Langerhans cell density of 1 x 10^3 cells/mm^2 and a keratinocyte density of 1.27 x 10^6 cells/mm^3 (Table 1), this results in an epidermal cell density of 1.3 x 10^6 cells/mm^3 including both keratinocytes and Langerhans cells. Dermal dendritic cells have been reported to make up 7% of the total dermal cell population (Dupasquier et al., 2004). Assuming 110 dermal dendritic cells per mm^2, this results in a total cell density of 6.2 x 10^4 cells/mm^3. It was assumed that all cells present in the skin can bind antigens, therefore, all skin cells were included in the cell density. The range of values for the

number of receptors per cell was 1 x 10^2 to 1.7 x 10^6, which reflect values reported in the literature (Table 1).

Multiplying the range of receptors per cell and the calculated total cell densities in the epidermis and dermis, the receptor density was determined to range from 6.2 x 10^6 to 2.2 x 10^{12} receptors/mm^3. Using the Avogadro constant, this corresponds to an initial receptor concentration R_{tot} of 1.0 x 10^{-11} to 3.7 x 10^{-6} µmol/mm^3.

Table 1: Kinetic parameter values from the literature for various compounds and the range of values used in the current study. The values from literature have been measured in various species.

	Value in literature	Related to	Range used in current study
k_a [M^{-1} s^{-1}]	2 x 10^5	Antigen (ovalbumin) to antibody (antiovalbumin)[1]	1 x 10^4 to 1 x 10^7
	1.4 x 10^5 to 8.1 x 10^5	Antigen (2,4-dinitrophenyl guinea pig albumin ($DNP_{16}GPA$)) to lymphocytes[2]	
	1 x 10^4 to 3 x 10^7	Various ligands and receptors[3]	
	1.2 x 10^4 to 3.3 x 10^5	Diphtheria toxoids to antibodies[4]	
k_d [s^{-1}]	1 x 10^{-3}	Antigen (ovalbumin) to antibody (antiovalbumin)[1]	1 x 10^{-7} to 1 x 10^{-3}
	1 x 10^{-7} to 1.9 x 10^{-6}	Antigen (2,4-dinitrophenyl guinea pig albumin ($DNP_{16}GPA$)) to lymphocytes[2]	
	2.5 x 10^{-5} to 4 x 10^{-1}	Various ligands and receptors[3]	
	1.8 x 10^{-4} to 5.6 x 10^{-3}	Diphtheria toxoids to antibodies[4]	
k_{int} [s^{-1}]	1.7 x 10^{-3} to 1.2 x 10^{-2}	Receptor-mediated endocytosis of epidermal growth factor (EGF) by Balb/c 3T3 cells[5]	1 x 10^{-4} to 1 x 10^{-2}
	1.1 x 10^{-4} to 1.4 x 10^{-3}	Internalization of various antibodies, ligands and receptors[6]*	
	1.2 x 10^{-4} to 2.2 x 10^{-3}	Endocytosis of dipotassium salt by murine dendritic cells from mice spleen[7]*	
k_c [s^{-1}]	0.9 x 10^{-5} to 1.2 x 10^{-3}	Model fit to data of various compounds[8]	1 x 10^{-6} to 1 x 10^{-2}
	0.9 x 10^{-4} to 1.4 x 10^{-3}	Model fit to data of various compounds[9]	
	2.5 x 10^{-3} to 1 x 10^{-2}	Used in skin model, no experiments[10]	
	5 x 10^{-6} to 5 x 10^{-5}	Used in skin model, theoretical values[11]	
N_{rec} [receptors/cell]	1 x 10^2 to 2 x 10^3	Toll-like receptors 1 and 4 on human monocytes and (im)mature dendritic cells[12]	1 x 10^2 to 1.7 x 10^6
	1.7 x 10^6	Sugar receptors on human $CD1a^+$ dendritic cells from blood[13]	
	1 x 10^4	Mammose receptor on human keratinocytes[14]	
	2 x 10^3 to 7 x 10^3	Toll-like receptors 2 on human monocytes[15]	
n_{cell} [cells/mm^2]	4 x 10^2 to 1 x 10^3	Langerhans cells in human epidermis[16,17,18,19,20]	1 x 10^3 Langerhans cells in epidermis
	1.1 x 10^2	Dermal dendritic cells in human dermis[21]	1.1 x 10^2 dendritic cells in dermis
	2 x 10^2	Dermal dendritic cells in mice dermis[22]	
N_{cell} [cells/mm^3]	1.27 x 10^6	Keratinocytes in mice epidermis[23]	1.27 x 10^6 keratinocytes in epidermis
t_r [s]	10	Delivery of influenza vaccine with coated MN[24]	10 to 3.6 x 10^3

6×10^2	Delivery of influenza vaccine with coated MN[25]
3.6×10^3	Delivery of ovalbumin with coated MN[26]

[1] (Dandliker and Levison, 1968); [2] (Davie and Paul, 1972); [3] (Lauffenburger and Linderman, 1993); [4] (Metz et al., 2003); [5] (Gex-Fabry and DeLisi, 1984); [6] (Vainshtein et al., 2015); [7] (Levine and Chain, 1992); [8] (Ibrahim et al., 2012); [9] (Kretsos et al., 2008); [10] (Lv et al., 2006); [11] (Guy and Hadgraft, 1983); [12] (Visintin et al., 2001); [13] (Avraméas et al., 1996); [14] (Szolnoky et al., 2001); [15] (Orihara et al., 2007) [16] (Liard et al., 2012); [17] (Stoitzner et al., 1999); [18] (Berman et al., 1983); [19] (Chen et al., 1985); [20] (Yu et al., 1994); [21] (McLellan et al., 1998); [22] (Ng et al., 2008); [23] (Mulholland et al., 2006); [24] (Fernando et al., 2012); [25] (Kim et al., 2010); [26] (Matriano et al., 2002)
**A half-time $t_{1/2}$ has been reported in the reference, this was converted to a rate constant using $k_{int} = ln(2)\ /t_{1/2}$.*

2.2.3 Antigen dose and release

Two doses of antigens were considered during the simulations. The first dose was based on the clinical dose used for human diphtheria vaccination. Using values reported in literature (Metz et al., 2003; World Health Organization (WHO), 2013), this dose was calculated to be 9 µg of diphtheria toxoid (DT). With a molecular weight of DT of 58 kDa (Metz et al., 2003) and considering a microneedle array containing 25 microneedles, this results in a dose of 6.2×10^{-6} µmol per microneedle. This dose for a single microneedle was assumed in the model and is hereafter referred to as high dose. The second dose was based on the dose that induces an immune response in mice, and was 0.3 µg DT (Schipper, Bouwstra, unpublished data). This results in a dose of 2.07×10^{-7} µmol per microneedle, hereafter called low dose. In both cases, various doses between +20% and -20% of the distinct dose were used as input values for the sensitivity study. These doses represent the initial antigen concentration in the microneedle compartment $C_{MN,0}$ from which the antigens are released into the ECM.

Table 1 also summarizes the required time period for release from a coated microneedle as reported in the literature. In the simulations, the antigen release from the coated microneedle, and thus the release of antigens to the skin ECM compartment, was assumed to be occur within 10 to 3600 seconds (t_r = 10 to 3600 s).

2.3 Sensitivity analysis

To evaluate the influence of the model parameters on the uncertainty in the model output, a global, variance-based sensitivity analysis was performed (Crestaux et al., 2009; Huberts et al., 2014). More specifically, for each parameter, its contribution to the total variance in the model output was estimated. This was done by dividing the total variance into various components. One main component for each parameter and supplementary components representing the interaction between two or more parameters. The ratio between the main component of a single parameter to the total variance of the output is expressed as the main sensitivity index of that parameter S_i. In addition, the total sensitivity index $S_{T,i}$ of a parameter is its total contribution, the sum of its main and supplementary components, to the variance normalized by the total variance of the output. The sum of all main sensitivity indices is equal or smaller than 1 by definition, whereas the sum of the total sensitivity

indices is equal or larger than 1 (Sobol', 2001). A large main sensitivity index of a parameter indicates that the parameter has a major influence on the model outcome, and should therefore receive priority to be measured accurately (parameter prioritization). In addition, a parameter with a small total sensitivity index may be fixed within its uncertainty range (parameter fixing), since it has little influence on the output of the model (Huberts et al., 2013; Saltelli et al., 2004).

The sensitivity analysis made use of generalized polynomial chaos expansion (Crestaux et al., 2009; Huberts et al., 2014). First, sets of input samples, obtained within the specified ranges using a quasi-random Sobol sequence, were used to perform multiple model runs and thereby sample the output spaces. Subsequently, to describe these output spaces, metamodels were constructed in the form of polynomials that are a function of the input parameters. Finally, the sensitivity indices are analytically derived from the metamodels. The method has been previously detailed and evaluated (Donders et al., 2015; Huberts et al., 2014), and has been recently applied to a constitutive model (van Kempen et al., 2015). The quality of the metamodels was assessed by calculating the coefficient of determination R^2 and the validation coefficient Q^2 (Donders et al., 2015).

During the analysis, the influence of the input parameters ($C_{MN,0}$, t_r, k_a, k_d, k_{int}, k_c, and R_{tot}) on the variation of the equilibrium concentrations in both the circulation C_{circ} and the cell C_{cell} were determined. The concentration in the other compartments can be considered to be zero at equilibrium, hence these are not of interest as output. The analysis was performed for both the low and high doses. For the analysis, 1650 model runs were performed.

3. Results

3.1 Progress of concentrations in the various compartments

Depending on the exact model parameters, most simulations reach equilibrium within 100 minutes for both low and high doses. Typical examples of the kinetics in the skin are shown in Figure 2. In these simulations, the arithmetic and geometric mean of the model parameter ranges were used in both dose cases, with the former defined as $(i_{min} + i_{max})/2$ and the latter as $\sqrt{i_{min} i_{max}}$, with i_{min} the minimal value in the range of parameter i and i_{max} its maximal value. The values are listed in Table 2. The process of the kinetics in the skin was dependent on the model parameters. In both examples with a high dose (Fig. 2a and b), the uptake of antigens by the cells was saturated at equilibrium, that is, the concentration in the cells C_{cell} is equal to the initial concentration of receptors R_{tot}. In the cases of a low dose (Fig. 2c and d), the cellular uptake was only saturated in one of the cases (Fig. 2d). However, for the other example with low dose the antigen uptake by the cells did not reach its maximum (Fig. 2c). Therefore, less cells will be activated in this case compared to the same model with a high dose (Fig. 2a). Nevertheless, at high dose more antigens end up in the circulation, as can be seen by the higher concentration in the circulation C_{circ} (Fig. 2a and c), which may be inefficient.

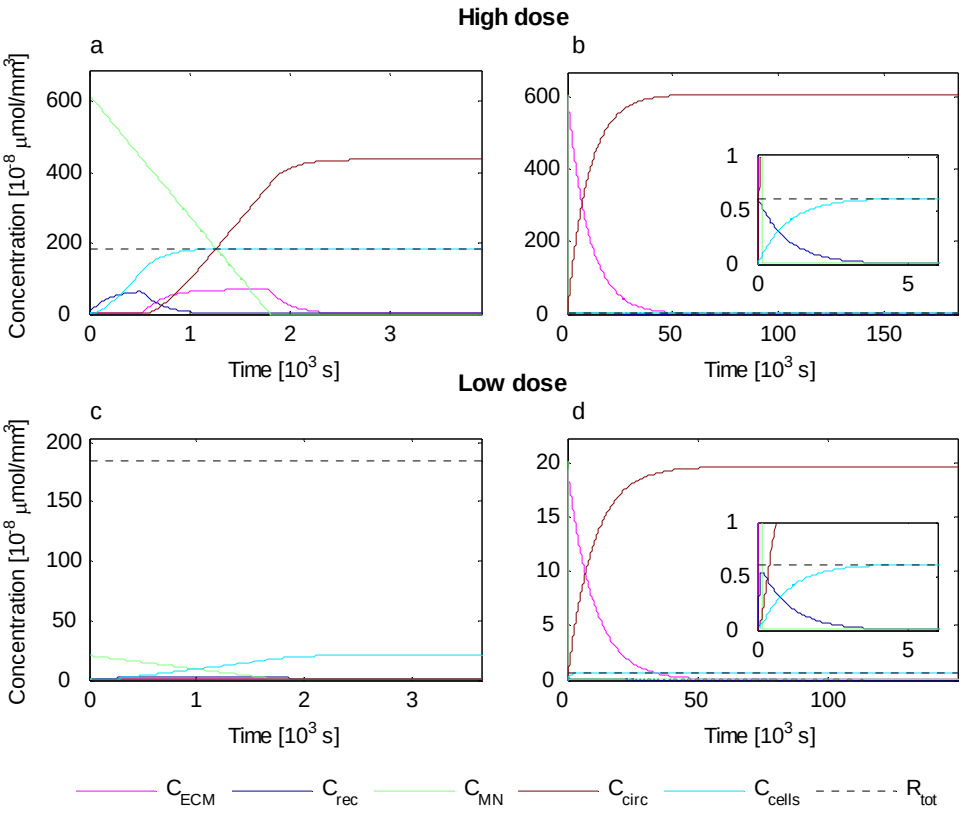

Figure 2. Four examples of the change in concentration in the various compartments of the skin during and after release of an antigen from a microneedle. (a) and (c) represent the simulations using the arithmetic mean of the parameter ranges with a high (a) and low (c) dose (Table 2). (b) and (d) represent the simulation using the geometric mean of the parameter ranges with a high (b) and low (d) dose. In addition to the concentrations in the compartments, the initial receptor concentration R_{tot} is shown to illustrate the level of full saturation of the cell compartment. The inlays in the figures (b) and (d) are a close-up of the main figure.

Table 2. Values of model parameters as used for the simulations used in Figure 2. For both the high dose and low dose cases, the arithmetic and geometric mean of the parameter ranges was used as input.

	Values of model parameter							
	Low dose $C_{MN,0}$ [µmol/mm^3]	High dose $C_{MN,0}$ [µmol/mm^3]	t_r [s]	k_a [M^{-1}s^{-1}]	k_d [s^{-1}]	k_{int} [s^{-1}]	k_c [s^{-1}]	R_{tot} [rec/mm^3]
Arithmetic mean	2.07 x 10^{-7}	6.21 x 10^{-6}	1.80 x 10^3	5.00 x 10^6	5.00 x 10^{-4}	5.05 x 10^{-3}	5.00 x 10^{-3}	1.85 x 10^{-6}
Geometric mean	2.03 x 10^{-7}	6.08 x 10^{-6}	1.90 x 10^2	3.16 x 10^5	1.00 x 10^{-5}	1.00 x 10^{-3}	1.00 x 10^{-4}	6.08 x 10^{-9}

3.2 Saturation of cells and distribution between compartments

The simulations, which were run for the sensitivity analysis, also provide a general overview of the saturation of the cells to internalize antigens. For the high dose at equilibrium, the cells were at least close to saturation (>99%) in 94% of the simulations. Due to the model definition, the highest possible equilibrium concentration in the cells is equal to the concentration of receptors R_{tot} or the initial antigen concentration in the microneedle $C_{MN,0}$, depending on which of the two values is the lowest. In all high dose simulations, the concentration of receptors was lower than the initial antigen concentration, therefore the cells could maximally reach a concentration equal to the receptor concentration. Apparently, the rate of internalization of antigens was fast enough compared to the

rate of uptake in the circulation to reach this maximum for 94% of the simulations, and thus the cells were saturated. By contrast, in the case of a low dose, the receptor concentration was often higher than the initial antigen concentration, resulting in the antigen saturation (>99%) of the cells for only 5% of the simulations.

Moreover, the distribution of the antigens at equilibrium was different for the high and low doses (Fig. 3). In most of the simulations at high dose, more than 50% of the antigens ended up in the circulation (Fig. 3a), while for low doses, more than 90% of the antigens were internalized into the cells for the majority of the simulations (Fig. 3b). This can again be attributed to the ratio of the dose and concentration of receptors and, consequently, the saturation of the cells.

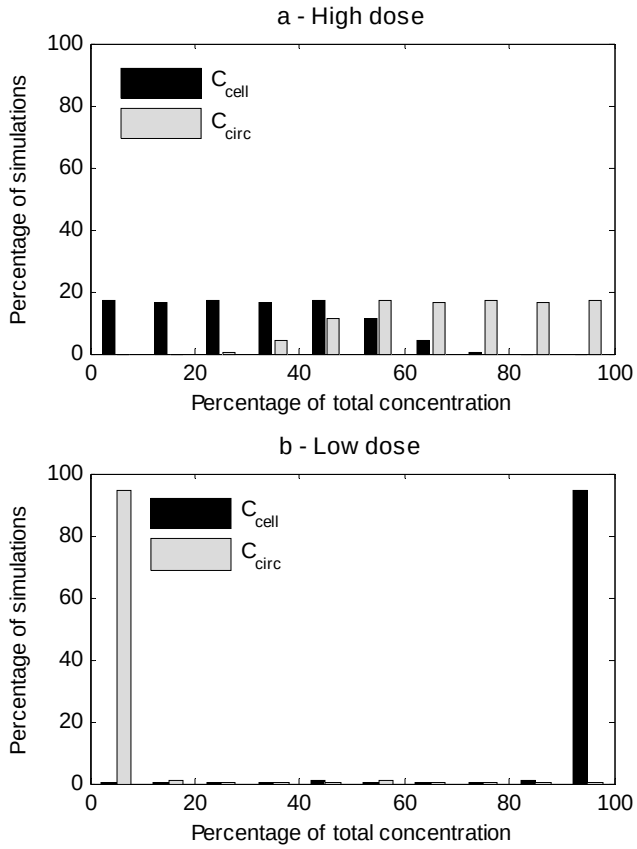

Figure 3. Distribution of the antigens between the intracellular and circulation compartments at equilibrium presented in the percentage of the total concentration and percentage of simulations for the simulations with a high (a) and low (b) dose.

3.3 Sensitivity analysis

The influence of the various model parameters on the uncertainty of the model output was assessed with a sensitivity analysis. A descriptive analysis of the equilibrium concentration in the cells and circulation is detailed in Table 3. The contribution of each parameter to this variance was determined and is presented as the main and total sensitivity indices (Fig. 4 and 5). The metamodels were able to describe the model outputs (R^2 = 0.85 to 1.00) and had a good predictive power (Q^2 = 0.70 to 0.99),

except for the variance in the concentration of the circulation at low dose. For this case the quality of the metamodel was less (R^2 = 0.75, and Q^2 = 0.51).

Table 3. The mean, variance, minimum and maximum value of the equilibrium concentration in the cells and circulation for the simulations performed for the sensitivity analysis. The values for both high and low dose are presented.

	Mean [μmol/mm^3]	Variance [(μmol/mm^3)^2]	Minimum [μmol/mm^3]	Maximum [μmol/mm^3]
High dose				
$C_{cells,eq}$	1.85 x 10^{-6}	1.14 x 10^{-12}	1.00 x 10^{-11}	3.70 x 10^{-6}
$C_{circ,eq}$	4.36 x 10^{-6}	1.66 x 10^{-12}	1.41 x 10^{-6}	7.32 x 10^{-6}
Low dose				
$C_{cells,eq}$	2.00 x 10^{-7}	1.31 x 10^{-15}	1.00 x 10^{-11}	2.48 x 10^{-7}
$C_{circ,eq}$	6.71 x 10^{-9}	8.06 x 10^{-16}	2.97 x 10^{-13}	2.32 x 10^{-7}

The variance of the final concentration in the cells was almost entirely determined by the receptor concentration R_{tot} for the high dose, indicated by the large main and total sensitivity indices (Fig. 4a). For the low dose, the variance was mainly determined by the receptor concentration R_{tot} (Fig. 4b). In addition, the initial concentration $C_{MN,0}$ contributed to the variance of the intracellular concentration. This can be explained by the fact that the maximal concentration in the cells is restricted by the concentration of receptors or the initial concentration. It is interesting to note that, the rate constants and release time contributed little to the variance in the output, as indicated by the low sensitivity indices (Fig. 4a and b). The sum of the main indices was close to one for the high dose, indicating that interactions between model parameters did not contribute to the total variance. A slight contribution of these higher-order effects was seen in case of a low dose.

In a similar manner to the intracellular concentration, the variation in the equilibrium concentration of the circulation was dominated by the receptor concentration and initial concentration of the microneedle (Fig. 5). Again, the rate constants and release period provide minor contributions to the low dose case alone (Fig. 5b), however, it should be noted that in this case the quality of the metamodel to describe the model output was poor.

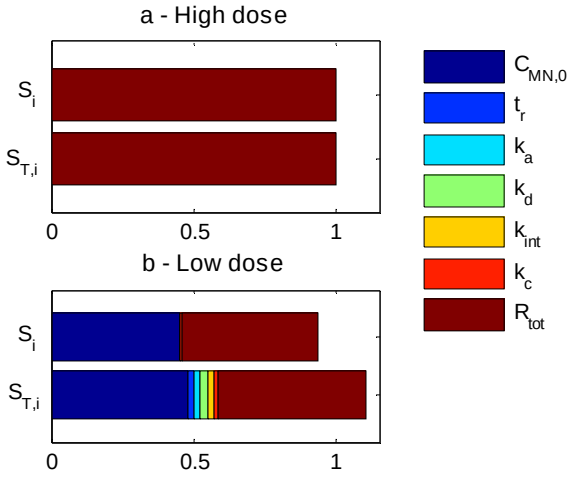

Figure 4. The main (S_i) and total ($S_{T,i}$) sensitivity indices of the model parameters for the equilibrium concentration in the cells, resulting from the sensitivity analysis. The indices for a high (a) and low (b) dose were determined.

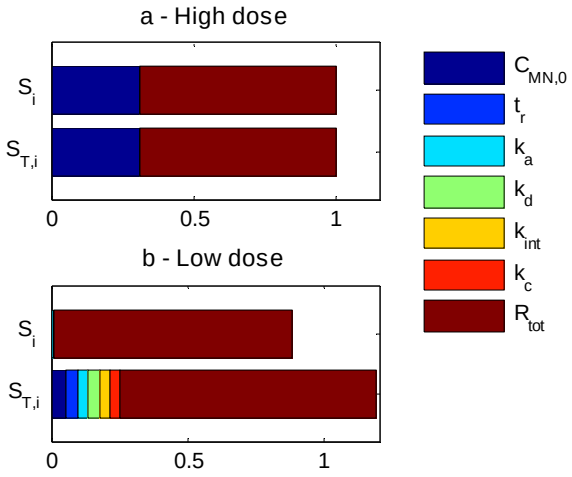

Figure 5. The main (S_i) and total ($S_{T,i}$) sensitivity indices of the model parameters for the equilibrium concentration in the circulation, resulting from the sensitivity analysis. The indices for a high (a) and low (b) dose were determined.

4. Discussion

Devices to deliver a vaccine intradermally, such as microneedle arrays, may be optimized in such a way as to activate a maximal number of APCs, which can subsequently initiate the adaptive immune response. The kinetics in the skin was described after antigen delivery using a theoretical compartment model, which included binding and internalization of the antigens by cells. In the case of a high administered dose (9 µg of diphtheria toxoid), the uptake of antigens by cells was saturated for the majority of model parameter combinations, in contrast to a lower dose of 0.3 µg DT. This discrepancy could be explained by the difference in proportion of the administered dose to the initially available binding sites for the antigens on the surface of the cells. When the cells were saturated, the rest of the antigens were delivered into the circulation. This represented more than 50% of the total antigens in the majority of the simulations with a high dose (Fig. 3), and may result in the dissipation of antigens. Hence, the dose should be adapted to the number of binding sites to minimize dissipation. A sensitivity

analysis confirmed that the initial concentration of receptors and the delivered dose were the two parameters that mainly influenced the variation in equilibrium concentration of the cells and circulation. These two parameters will have to be measured accurately to be able to validate the developed model.

In the current model, the initial receptor concentration was based on the number of cells initially present in the skin and the amount of receptors on the cell membrane of a single cell. This initial concentration indirectly prescribed the maximal amount of antigens that could be internalized by the cells. However, in preclinical or clinical studies, additional processes may play a role that increase the concentration of antigen binding sites. First, upon antigen delivery, cells residing in the skin start to produce cytokines and chemokines (Abbas et al., 2012; Koutsonanos et al., 2013; Ueno et al., 2007). These signal molecules attract additional immune cells, including dendritic cells, towards the site of delivery or stimulate proliferation and, thereby, increase the total number of cells available in the skin (Del Pilar Martin et al., 2012; Koutsonanos et al., 2013). Secondly, depending on the type of receptors, they may return to the cell membrane after facilitating the uptake of an antigen (Mizuno et al., 2004; Sallusto et al., 1995). This recycling process was modelled in more detail by Gex-Fabry et al. (Gex-Fabry and DeLisi, 1984). However, in the current model it was assumed that a receptor was internalized together with a single antigen and was not recycled, which is the case for certain types of receptors. Since, the number of receptors is an important factor in the antigen distribution within the skin, the migration of cells to the skin, the recycling of receptors, and the change in receptor expression will have to be included in future studies to obtain a more complete view on the skin kinetics. Moreover, uptake of antigens via pinocytosis may be incorporated in future models. In the current study, the differences between dermal dendritic cells, Langerhans cells, and other cells in, among others, receptor types, efficiency in antigen capture, and efficiency to initiate an immune response were not specifically considered. However, the differences will most probably lie within the parameter ranges. In addition, in the current model, the intracellular concentration was assumed to be an important output for both cell activation and the subsequent immune response. However, the signalling between cells also stimulates the activation and migration of APCs (Del Pilar Martin et al., 2012). Thus, antigen uptake by the cells is not the only trigger for an APC to migrate to the lymph nodes. It is not evident that the initiated immune response increases with an increased antigen saturation of the antigen presenting cells. However, it is likely that the response of the cells towards maturation correlates to intracellular antigen levels. Larger numbers of migrating cells will in turn increase the antigen presentation to T-cells.

The results suggest that the dose applied to the skin should be adapted to the amount of cells and receptors for a specific compound and the size of the area of application, in such a way that the majority of the APCs are activated, but antigens are not lost to the circulation. On the other hand,

losing antigens to the lymphatic circulation may not be a disadvantage when these antigens are directly transported to the lymph nodes and activate lymph-node resident dendritic cells. When it is taken into account that cells are recruited to the skin to repopulate it, in some situations, it may be more beneficial to apply multiple low doses over a longer period of time as opposed to a single high dose. Indeed such a regimen was shown to induce a stronger immune response in mice (Johansen et al., 2008). In the current model, a constant release from the microneedle compartment was considered as opposed to an exponential release. The type of release will mainly influence the release time, which had no effect on the final distribution between the compartments. Hence, the type of release will not influence the findings. In the case where long-term effects would be incorporated into the model, the release rate may prove to be of importance.

Values for the model parameters were taken from a comprehensive range presented in the literature, involving measurements in both mice and human, skin and non-skin cells, and for various compounds and receptors (Table 1). Using these ranges of values, the variance in the model outputs was quite large (Table 3). However, the sensitivity analysis provided insight into which parameters have a large influence on these variances. The results revealed that the initial receptor concentration R_{tot} and the initial concentration $C_{MN,0}$ are parameters that should be measured to validate and use the model for a specific compound and/or species, since they demonstrate high main sensitivity indices (Fig. 4 and 5), indicating that they have a large influence on the uncertainty of the model outcome. By contrast, the other parameters, demonstrating a relatively low total sensitivity index, may be based on general values reported in the literature. Several methods exist to determine the amount of receptors on a cell. Previous studies have used fluorescently labelled molecules that bind to receptors in combination with flow cytometry (Avraméas et al., 1996; Orihara et al., 2007; Visintin et al., 2001). Others used labelled ligands with a radioactive label and subsequently determined the radioactivity of the cells (Szolnoky et al., 2001) to derive the amount of receptors per cell. Hence, it is possible to determine this important parameter for a specific application.

The spatial distribution of antigens in the skin was currently not modelled. Such a model would account for differences in cell density, receptor type, and antigen capturing capacity of dermal dendritic cells and Langerhans cells, which can subsequently influence the amount of antigens taken up by these cells. This can be of interest, because these cells may induce a different immune response. In addition, the diffusion of antigens and their transport via the microcirculation can influence the amount of cells that can be reached. Indeed, previous studies reported both of these factors are important for the distribution within the skin and its deeper layers (Anissimov and Roberts, 2011; Dancik et al., 2012).

The present model has the potential to be extended to incorporate the spatial distribution of antigens, geometries of microneedles and microneedle arrays, and variations in properties of the various skin layers. However, to use the model for specific applications, it is important to first validate the model

with in vivo experiments. An extended model will result in a computational method to facilitate the design of microneedle arrays, able to induce a highly effective immune response.

Acknowledgements

We thank Wouter Donders from Maastricht University for his help with the sensitivity analysis. Moreover, we thank Pim Schipper from the Leiden Academic Centre for Drug Research of Leiden University for his contribution in the discussions. This research is supported by the Dutch Technology Foundation STW, which is part of the Netherlands Organisation for Scientific Research (NWO), and which is partly funded by the Ministry of Economic Affairs (Project no. 11259).

References

Abbas, A.K., Lichtman, A.H., Pillai, S., 2012. Basic Immunology, 4th ed. Elsevier Health Sciences.

Al-Qallaf, B., Das, D.B., Davidson, A., 2009. Transdermal drug delivery by coated microneedles: geometry effects on drug concentration in blood. Asia-Pac. J. Chem. Eng. 4, 845–857. doi:10.1002/apj.353

Al-Zahrani, S., Zaric, M., McCrudden, C., Scott, C., Kissenpfennig, A., Donnelly, R.F., 2012. Microneedle-mediated vaccine delivery: harnessing cutaneous immunobiology to improve efficacy. Expert Opin. Drug Deliv. 9, 541–550. doi:10.1517/17425247.2012.676038

Anissimov, Y., Roberts, M., 2011. Modelling Dermal Drug Distribution After Topical Application in Human. Pharm. Res. 28, 2119–2129. doi:10.1007/s11095-011-0437-2

Avraméas, A., McIlroy, D., Hosmalin, A., Autran, B., Debré, P., Monsigny, M., Roche, A.C., Midoux, P., 1996. Expression of a mannose/fucose membrane lectin on human dendritic cells. Eur. J. Immunol. 26, 394–400. doi:10.1002/eji.1830260219

Berman, B., Chen, V.L., France, D.S., Dotz, W.I., Petroni, G., 1983. Anatomical mapping of epidermal Langerhans cell densities in adults. Br. J. Dermatol. 109, 553–558. doi:10.1111/j.1365-2133.1983.tb07678.x

Bos, J.D., Meinardi, M.M.H.M., 2000. The 500 Dalton rule for the skin penetration of chemical compounds and drugs. Exp. Dermatol. 9, 165–169. doi:10.1034/j.1600-0625.2000.009003165.x

Carey, J.B., Pearson, F.E., Vrdoljak, A., McGrath, M.G., Crean, A.M., Walsh, P.T., Doody, T., O'Mahony, C., Hill, A.V.S., Moore, A.C., 2011. Microneedle array design determines the induction of protective memory CD8+ T cell responses induced by a recombinant live malaria vaccine in mice. PloS One 6, e22442. doi:10.1371/journal.pone.0022442

Chen, H., Yuan, J., Wang, Y., Silvers, W. k., 1985. Distribution of ATPase-positive Langerhans cells in normal adult human skin. Br. J. Dermatol. 113, 707–711. doi:10.1111/j.1365-2133.1985.tb02406.x

Crestaux, T., Le Maître, O., Martinez, J.-M., 2009. Polynomial chaos expansion for sensitivity analysis. Reliab. Eng. Syst. Saf. 94, 1161–1172. doi:10.1016/j.ress.2008.10.008

Dancik, Y., Anissimov, Y.G., Jepps, O.G., Roberts, M.S., 2012. Convective transport of highly plasma protein bound drugs facilitates direct penetration into deep tissues after topical application. Br. J. Clin. Pharmacol. 73, 564–578. doi:10.1111/j.1365-2125.2011.04128.x

Dandliker, W.B., Levison, S.A., 1968. Investigation of antigen-antibody kinetics by fluorescence polarization. Immunochemistry 5, 171–183. doi:10.1016/0019-2791(68)90101-8

Davie, J.M., Paul, W.E., 1972. Receptors on Immunocompetent Cells Iv. Direct Measurement of Avidity of Cell Receptors and Cooperative Binding of Multivalent Ligands. J. Exp. Med. 135, 643–659. doi:10.1084/jem.135.3.643

Del Pilar Martin, M., Weldon, W.C., Zarnitsyn, V.G., Koutsonanos, D.G., Akbari, H., Skountzou, I., Jacob, J., Prausnitz, M.R., Compans, R.W., 2012. Local response to microneedle-based influenza immunization in the skin. mBio 3, e00012–12. doi:10.1128/mBio.00012-12

Depelsenaire, A.C.I., Meliga, S.C., McNeilly, C.L., Pearson, F.E., Coffey, J.W., Haigh, O.L., Flaim, C.J., Frazer, I.H., Kendall, M.A.F., 2014. Colocalization of cell death with antigen deposition in skin enhances vaccine immunogenicity. J. Invest. Dermatol. 134, 2361–2370. doi:10.1038/jid.2014.174

Donders, W.P., Huberts, W., van de Vosse, F.N., Delhaas, T., 2015. Personalization of models with many model parameters: an efficient sensitivity analysis approach. Int. J. Numer. Methods Biomed. Eng. 31, e02727. doi:10.1002/cnm.2727

Dupasquier, M., Stoitzner, P., van Oudenaren, A., Romani, N., Leenen, P.J.M., 2004. Macrophages and dendritic cells constitute a major subpopulation of cells in the mouse dermis. J. Invest. Dermatol. 123, 876–879. doi:10.1111/j.0022-202X.2004.23427.x

Dzopalic, T., Rajkovic, I., Dragicevic, A., Colic, M., 2012. The response of human dendritic cells to co-ligation of pattern-recognition receptors. Immunol. Res. 52, 20–33. doi:10.1007/s12026-012-8279-5

Fernando, G.J.P., Chen, X., Primiero, C.A., Yukiko, S.R., Fairmaid, E.J., Corbett, H.J., Frazer, I.H., Brown, L.E., Kendall, M.A.F., 2012. Nanopatch targeted delivery of both antigen and adjuvant to skin synergistically drives enhanced antibody responses. J. Controlled Release 159, 215–221. doi:10.1016/j.jconrel.2012.01.030

Flacher, V., Bouschbacher, M., Verronèse, E., Massacrier, C., Sisirak, V., Berthier-Vergnes, O., de Saint-Vis, B., Caux, C., Dezutter-Dambuyant, C., Lebecque, S., Valladeau, J., 2006. Human langerhans cells express a specific TLR profile and differentially respond to viruses and gram-positive bacteria. J. Immunol. 177, 7959–7967. doi:10.4049/jimmunol.177.11.7959

Gex-Fabry, M., DeLisi, C., 1984. Receptor-mediated endocytosis: a model and its implications for experimental analysis. Am. J. Physiol. - Regul. Integr. Comp. Physiol. 247, R768–R779.

Giese, M., 2013. Basic vaccine immunology, in: Giese, M. (Ed.), Molecular Vaccines. Springer Vienna, pp. 23–58.

Guy, R.H., Hadgraft, J., 1983. Physicochemical interpretation of the pharmacokinetics of percutaneous absorption. J. Pharmacokinet. Biopharm. 11, 189–203. doi:10.1007/BF01061849

Huberts, W., de Jonge, C., van der Linden, W.P.M., Inda, M.A., Tordoir, J.H.M., van de Vosse, F.N., Bosboom, E.M.H., 2013. A sensitivity analysis of a personalized pulse wave propagation model for arteriovenous fistula surgery. Part A: identification of most influential model parameters. Med. Eng. Phys. 35, 810–826. doi:10.1016/j.medengphy.2012.08.013

Huberts, W., Donders, W.P., Delhaas, T., van de Vosse, F.N., 2014. Applicability of the polynomial chaos expansion method for personalization of a cardiovascular pulse wave propagation model. Int. J. Numer. Methods Biomed. Eng. 30, 1679–1704. doi:10.1002/cnm.2695

Ibrahim, R., Nitsche, J.M., Kasting, G.B., 2012. Dermal clearance model for epidermal bioavailability calculations. J. Pharm. Sci. 101, 2094–2108. doi:10.1002/jps.23106

Indermun, S., Luttge, R., Choonara, Y.E., Kumar, P., du Toit, L.C., Modi, G., Pillay, V., 2014. Current advances in the fabrication of microneedles for transdermal delivery. J. Controlled Release 185, 130–138. doi:10.1016/j.jconrel.2014.04.052

Johansen, P., Storni, T., Rettig, L., Qiu, Z., Der-Sarkissian, A., Smith, K.A., Manolova, V., Lang, K.S., Senti, G., Müllhaupt, B., Gerlach, T., Speck, R.F., Bot, A., Kündig, T.M., 2008. Antigen kinetics determines immune reactivity. Proc. Natl. Acad. Sci. 105, 5189–5194. doi:10.1073/pnas.0706296105

Kim, K.S., Ita, K., Simon, L., 2015. Modelling of dissolving microneedles for transdermal drug delivery: theoretical and experimental aspects. Eur. J. Pharm. Sci. 68, 137–143. doi:10.1016/j.ejps.2014.12.008

Kim, Y.-C., Park, J.-H., Prausnitz, M.R., 2012. Microneedles for drug and vaccine delivery. Adv. Drug Deliv. Rev. 64, 1547–1568. doi:10.1016/j.addr.2012.04.005

Kim, Y.-C., Quan, F.-S., Compans, R.W., Kang, S.-M., Prausnitz, M.R., 2010. Stability kinetics of influenza vaccine coated onto microneedles during drying and storage. Pharm. Res. 28, 135–144. doi:10.1007/s11095-010-0134-6

Koutsonanos, D.G., Compans, R.W., Skountzou, I., 2013. Targeting the skin for microneedle delivery of influenza vaccine, in: Katsikis, P.D., Schoenberger, S.P., Pulendran, B. (Eds.), Crossroads between Innate and Adaptive Immunity IV, Advances in Experimental Medicine and Biology. Springer New York, pp. 121–132.

Kretsos, K., Miller, M.A., Zamora-Estrada, G., Kasting, G.B., 2008. Partitioning, diffusivity and clearance of skin permeants in mammalian dermis. Int. J. Pharm. 346, 64–79. doi:10.1016/j.ijpharm.2007.06.020

Lauffenburger, D.A., Linderman, J.J., 1993. Receptors : models for binding, trafficking, and signaling. Oxford University Press, New York.

Levine, T.P., Chain, B.M., 1992. Endocytosis by antigen presenting cells: dendritic cells are as endocytically active as other antigen presenting cells. Proc. Natl. Acad. Sci. U. S. A. 89, 8342–8346.

Liard, C., Munier, S., Joulin-Giet, A., Bonduelle, O., Hadam, S., Duffy, D., Vogt, A., Verrier, B., Combadière, B., 2012. Intradermal immunization triggers epidermal langerhans cell mobilization required for CD8 T-cell immune responses. J. Invest. Dermatol. 132, 615–625. doi:10.1038/jid.2011.346

Lv, Y.-G., Liu, J., Gao, Y.-H., Xu, B., 2006. Modeling of transdermal drug delivery with a microneedle array. J. Micromechanics Microengineering 16, 2492–2501. doi:10.1088/0960-1317/16/11/034

Matriano, J.A., Cormier, M., Johnson, J., Young, W.A., Buttery, M., Nyam, K., Daddona, P.E., 2002. Macroflux microprojection array patch technology: a new and efficient approach for intracutaneous immunization. Pharm. Res. 19, 63–70.

McCarley, K.D., Bunge, A.L., 2001. Pharmacokinetic models of dermal absorption. J. Pharm. Sci. 90, 1699–1719.

McLellan, A.D., Heiser, A., Sorg, R.V., Fearnley, D.B., Hart, D.N.J., 1998. Dermal dendritic cells associated with T lymphocytes in normal human skin display an activated phenotype. J. Invest. Dermatol. 111, 841–849. doi:10.1046/j.1523-1747.1998.00375.x

Metz, B., Jiskoot, W., Hennink, W.E., Crommelin, D.J.A., Kersten, G.F.A., 2003. Physicochemical and immunochemical techniques predict the quality of diphtheria toxoid vaccines. Vaccine 22, 156–167. doi:10.1016/j.vaccine.2003.08.003

Mitragotri, S., Anissimov, Y.G., Bunge, A.L., Frasch, H.F., Guy, R.H., Hadgraft, J., Kasting, G.B., Lane, M.E., Roberts, M.S., 2011. Mathematical models of skin permeability: an overview. Int. J. Pharm. 418, 115–129. doi:10.1016/j.ijpharm.2011.02.023

Mizuno, K., Okamoto, H., Horio, T., 2004. Ultraviolet B radiation suppresses endocytosis, subsequent maturation, and migration activity of Langerhans cell-like dendritic cells. J. Invest. Dermatol. 122, 300–306. doi:10.1046/j.0022-202X.2004.22206.x

Mulholland, W.J., Arbuthnott, E.A.H., Bellhouse, B.J., Cornhill, J.F., Austyn, J.M., Kendall, M.A.F., Cui, Z., Tirlapur, U.K., 2006. Multiphoton high-resolution 3D imaging of Langerhans cells and keratinocytes in the mouse skin model adopted for epidermal powdered immunization. J. Invest. Dermatol. 126, 1541–1548. doi:10.1038/sj.jid.5700290

Naegel, A., Heisig, M., Wittum, G., 2013. Detailed modeling of skin penetration - An overview. Adv. Drug Deliv. Rev. 65, 191–207. doi:10.1016/j.addr.2012.10.009

Ng, L.G., Hsu, A., Mandell, M.A., Roediger, B., Hoeller, C., Mrass, P., Iparraguirre, A., Cavanagh, L.L., Triccas, J.A., Beverley, S.M., Scott, P., Weninger, W., 2008. Migratory dermal dendritic cells act as rapid sensors of protozoan parasites. PLoS Pathog. 4, e1000222. doi:10.1371/journal.ppat.1000222

Orihara, K., Nagata, K., Hamasaki, S., Oba, R., Hirai, H., Ishida, S., Kataoka, T., Oketani, N., Ogawa, M., Mizoguchi, E., Ichiki, H., Tei, C., 2007. Time-course of toll-like receptor 2 expression, as a predictor of recurrence in patients with bacterial infectious diseases. Clin. Exp. Immunol. 148, 260–270. doi:10.1111/j.1365-2249.2007.03352.x

Pearson, F.E., O'Mahony, C., Moore, A.C., Hill, A.V.S., 2015. Induction of CD8+ T cell responses and protective efficacy following microneedle-mediated delivery of a live adenovirus-vectored malaria vaccine. Vaccine 33, 3248–3255. doi:10.1016/j.vaccine.2015.03.039

Raphael, A.P., Meliga, S.C., Chen, X., Fernando, G.J.P., Flaim, C., Kendall, M.A.F., 2013. Depth-resolved characterization of diffusion properties within and across minimally-perturbed skin layers. J. Controlled Release 166, 87–94. doi:10.1016/j.jconrel.2012.12.010

Römgens, A.M., Bader, D.L., Bouwstra, J.A., Baaijens, F.P.T., Oomens, C.W.J., 2015. Diffusion profile of macromolecules within and between human skin layers for (trans)dermal drug delivery. J. Mech. Behav. Biomed. Mater. 50, 215–222. doi:10.1016/j.jmbbm.2015.06.019

Sallusto, F., Cella, M., Danieli, C., Lanzavecchia, A., 1995. Dendritic cells use macropinocytosis and the mannose receptor to concentrate macromolecules in the major histocompatibility complex class II compartment: downregulation by cytokines and bacterial products. J. Exp. Med. 182, 389–400.

Saltelli, A., Tarantola, S., Campolongo, F., Ratto, M., 2004. Sensitivity analysis in practice: a guide to assessing scientific models. John Wiley & Sons, Ltd., Chichester, West Sussex, UK.

Sobol', I.M., 2001. Global sensitivity indices for nonlinear mathematical models and their Monte Carlo estimates. Math. Comput. Simul. 55, 271–280. doi:10.1016/S0378-4754(00)00270-6

Stoitzner, P., Zanella, M., Ortner, U., Lukas, M., Tagwerker, A., Janke, K., Lutz, M.B., Schuler, G., Echtenacher, B., Ryffel, B., Koch, F., Romani, N., 1999. Migration of langerhans cells and dermal dendritic cells in skin organ cultures: augmentation by TNF-alpha and IL-1beta. J. Leukoc. Biol. 66, 462–470.

Szolnoky, G., Bata-Csörgö, Z., Kenderessy, A.S., Kiss, M., Pivarcsi, A., Novák, Z., Nagy Newman, K., Michel, G., Ruzicka, T., Maródi, L., Dobozy, A., Kemény, L., 2001. A mannose-binding receptor is expressed on human keratinocytes and mediates killing of Candida albicans. J. Invest. Dermatol. 117, 205–213. doi:10.1046/j.1523-1747.2001.14071.x

Ueno, H., Klechevsky, E., Morita, R., Aspord, C., Cao, T., Matsui, T., Di Pucchio, T., Connolly, J., Fay, J.W., Pascual, V., Palucka, A.K., Banchereau, J., 2007. Dendritic cell subsets in health and disease. Immunol. Rev. 219, 118–142. doi:10.1111/j.1600-065X.2007.00551.x

Vainshtein, I., Roskos, L.K., Cheng, J., Sleeman, M.A., Wang, B., Liang, M., 2015. Quantitative measurement of the target-mediated internalization kinetics of biopharmaceuticals. Pharm. Res. 32, 286–299. doi:10.1007/s11095-014-1462-8

van der Maaden, K., Jiskoot, W., Bouwstra, J., 2012. Microneedle technologies for (trans)dermal drug and vaccine delivery. J. Controlled Release 161, 645–655. doi:10.1016/j.jconrel.2012.01.042

van Kempen, T.H.S., Donders, W.P., van de Vosse, F.N., Peters, G.W.M., 2015. A constitutive model for developing blood clots with various compositions and their nonlinear viscoelastic behavior. Biomech. Model. Mechanobiol. doi:10.1007/s10237-015-0686-9

Visintin, A., Mazzoni, A., Spitzer, J.H., Wyllie, D.H., Dower, S.K., Segal, D.M., 2001. Regulation of toll-like receptors in human monocytes and dendritic cells. J. Immunol. 166, 249–255. doi:10.4049/jimmunol.166.1.249

Widera, G., Johnson, J., Kim, L., Libiran, L., Nyam, K., Daddona, P., Cormier, M., 2006. Effect of delivery parameters on immunization to ovalbumin following intracutaneous administration by a coated microneedle array patch system. Vaccine 24, 1653–1664. doi:10.1016/j.vaccine.2005.09.049

World Health Organization (WHO), 2013. Manual for quality control of diphtheria, tetanus and pertussis vaccines (No. WHO/IVB/11.11).

Yu, R.C., Abrams, D.C., Alaibac, M., Chu, A.C., 1994. Morphological and quantitative analyses of normal epidermal Langerhans cells using confocal scanning laser microscopy. Br. J. Dermatol. 131, 843–848. doi:10.1111/j.1365-2133.1994.tb08587.x

Zhang, R., Zhang, P., Dalton, C., Jullien, G.A., 2009. Modeling of drug delivery into tissues with a microneedle array using mixture theory. Biomech. Model. Mechanobiol. 9, 77–86. doi:10.1007/s10237-009-0160-7